

Entanglement entropy dynamics of non-Gaussian states in free boson systems: random sampling approach

Ryui Kaneko,^{1,*} Daichi Kagamihara,^{2,†} and Ippei Danshita^{3,‡}

¹*Physics Division, Sophia University, Chiyoda, Tokyo 102-8554, Japan*

²*Department of Physics, Chuo University, Bunkyo, Tokyo 112-8551, Japan*

³*Department of Physics, Kindai University, Higashi-Osaka, Osaka 577-8502, Japan*

(Dated: November 18, 2024)

We develop a random sampling method for calculating the time evolution of the Rényi entanglement entropy after a quantum quench from an insulating state in free boson systems. Because of the non-Gaussian nature of the initial state, calculating the Rényi entanglement entropy calls for the exponential cost of computing a matrix permanent. We numerically demonstrate that a simple random sampling method reduces the computational cost of a permanent; for an $N_s \times N_s$ matrix corresponding to N_s sites at half filling, the sampling cost becomes $O(2^{\alpha N_s})$ with a constant $\alpha \ll 1$, in contrast to the conventional algorithm with the $O(2^{N_s})$ number of summations requiring the exponential-time cost. Although the computational cost is still exponential, this improvement allows us to obtain the entanglement entropy dynamics in free boson systems for more than 100 sites. We present several examples of the entanglement entropy dynamics in low-dimensional free boson systems.

I. INTRODUCTION

Understanding dynamics of quantum many-body systems is a central issue in modern physics. The entanglement entropy is a key quantity to characterize the dynamics of quantum many-body systems. Previous studies have shown that the entanglement entropy provides information on the thermalization process and the propagation of quantum information [1–32]. Although the von Neumann entanglement entropy is not a directly measurable quantity, there are several proposals to measure Rényi entanglement entropy [33–35]. Recent experiments have successfully observed the dynamics of the Rényi entanglement entropy using ultracold atoms in optical lattices [36, 37] and trapped ions [38].

The numerical simulation of dynamics of the entanglement entropy is also an important approach to understanding quantum many-body systems and providing a benchmark for experiments. In contrast to the fermion and spin systems, the boson systems are much harder to simulate because of the large number of local Hilbert spaces. Even in the free boson systems with simple initial states, such as the Mott insulating state and the charge-density-wave (CDW) state, the entanglement entropy dynamics is difficult to calculate because of the non-Gaussian nature of the initial states. Although the analytical formula for the entanglement entropy is formally obtained by a matrix permanent, its numerical evaluation requires the exponential cost [30]. This situation limits the system size that can be studied to a few tens of sites or particles. Therefore, understanding dynamics of the entanglement entropy in boson systems remains to be a challenging problem even in noninteracting systems.

In this paper, we develop a random sampling method for calculating the time evolution of the Rényi entanglement entropy in free boson systems. In the developed method, we

still need to evaluate the matrix permanent, which requires the exponential computational cost in general. However, the growth rate of the computational cost is much slower than the exact permanent calculation. We have numerically found that the computational cost is reduced to $O(2^{\alpha N_s})$ with a small constant $\alpha \ll 1$ and the system size N_s . This improvement enables us to study dynamics of the entanglement entropy in free boson systems for more than 100 sites, confirming that the entanglement entropy in the long-time region exhibits the volume-law scaling as expected.

This paper is organized as follows: In Sec. II, we briefly review the calculation of the Rényi entanglement entropy in free boson systems and describe the conventional algorithm for evaluating the entanglement entropy, which requires the computation of a matrix permanent. To reduce the computational cost, we propose a random sampling method for the matrix permanent. In Sec. III, we examine the performance of the random sampling method by estimating the size dependence of the statistical error. We then present numerical results for dynamics of the entanglement entropy in free boson systems for spatial one (1D) and two dimensions (2D). Finally, in Sec. IV, we summarize our results and discuss future prospects. For simplicity, we set $\hbar = 1$ and take the lattice constant to be unity throughout this paper.

II. RANDOM SAMPLING METHOD FOR ENTANGLEMENT ENTROPY

We first briefly review how to evaluate time evolution of the Rényi entanglement entropy in free boson systems in the case that the initial state is an insulating state. Let us consider dynamics subjected to a quantum quench in the Bose-Hubbard model under the open boundary condition. The Hamiltonian is defined as

$$\hat{H} = -J \sum_{\langle j,l \rangle} (\hat{b}_j^\dagger \hat{b}_l + \text{H.c.}) + \sum_j \Omega_j \hat{n}_j + \frac{U}{2} \sum_j \hat{n}_j (\hat{n}_j - 1), \quad (1)$$

* ryuikaneko@sophia.ac.jp

† dkagamihara119@g.chuo-u.ac.jp

‡ danshita@phys.kindai.ac.jp

where the symbols \hat{b}_j and \hat{n}_j are the boson annihilation and number operators, respectively. The parameters J , U , and Ω_j represent the strength of the hopping, the strength of the interaction, and the single-particle potential, respectively. The symbol $\langle j, l \rangle$ means that sites j and l are nearest neighbors. We focus on a sudden quench from an insulating state to the noninteracting ($U = 0$) and homogeneous ($\Omega_j = 0$) point. As an initial state, we specifically choose the 010101 \dots -type CDW state at half filling. It is defined as

$$|\psi\rangle = \prod_{j \in A_{\text{CDW}}}^{N_s} \hat{b}_j^\dagger |0\rangle, \quad (2)$$

where $|0\rangle$ is the vacuum state of \hat{b}_j . The A_{CDW} corresponds to the set of charge rich sites. For example, $A_{\text{CDW}} = \{2, 4, 6, \dots\}$ in 1D, and $A_{\text{CDW}} = \{(2, 1), (4, 1), (6, 1), \dots, (1, 2), (3, 2), (5, 2), \dots, (2, 3), (4, 3), (6, 3), \dots, (1, 4), (3, 4), (5, 4), \dots\}$ in 2D, respectively. Hereafter, in 2D, we map the site index j ($= j_x + L_x j_y$) one-to-one to the lattice site (j_x, j_y) for $j_x = 1, 2, \dots, L_x$ and $j_y = 1, 2, \dots, L_y$ on a square lattice with L_x (L_y) being the length of the side along the x (y) direction, respectively. The number of sites is represented as N_s , which is taken as an even number in our study. Then, the number of particles is $N_b = N_s/2$. The CDW state can be obtained as the ground state of the Bose-Hubbard model at half filling for $\Omega/J \gg 1$ and $U/J \gg 1$ when $\Omega_j = \Omega(-1)^{j+1}$ in 1D and $\Omega_j = \Omega(-1)^{j_x+j_y}$ in 2D, respectively. One can prepare the CDW state in experiments using a secondary optical lattice, which has a lattice constant twice as large as that of the primary lattice [13]. Note that such CDW states and also the Mott insulating state that appear in the Bose-Hubbard model are non-Gaussian states, although the counterparts in the Fermi-Hubbard model are Gaussian states.

We previously obtained the Rényi entanglement entropy $S_2(t)$ of the time-evolved state, $|\psi(t)\rangle = \exp(-i\hat{H}t)|\psi\rangle$ [30]. At each time t , it is expressed as

$$S_2 = -\ln \text{perm}A, \quad (3)$$

$$A = \begin{pmatrix} Z & I - Z \\ I - Z & Z \end{pmatrix}. \quad (4)$$

Here, A is an $N_s \times N_s$ square matrix, I is an $N_s/2 \times N_s/2$ identity matrix, and the element $z_{i,j}(t)$ of an $N_s/2 \times N_s/2$ Hermitian matrix Z is given as

$$z_{i,j}(t) = \sum_{l \in A} y_{r_i,l}^*(t) y_{r_j,l}(t), \quad (5)$$

with r_i and r_j being indices of charge rich sites ($r_i, r_j \in A_{\text{CDW}}$). The symbol A in the subscript of summation denotes the subsystem that contains $l = 1, 2, \dots, N_A$ sites. For simplicity, we set N_A to half the system size ($N_A = N_s/2$) throughout this paper. The value $y_{i,j}(t)$ ($i, j = 1, 2, \dots, N_s$) is represented as

$$y_{i,j}(t) = \sum_{k=1}^{N_s} x_{k,i} x_{k,j} \exp(-i\epsilon_k t), \quad (6)$$

where ϵ_k and x_k are the k th eigenenergy and eigenstate of the noninteracting Hamiltonian in the first-quantization representation.

In general, the calculation of the matrix permanent in Eq. (3) requires the exponential cost of $O(N_s \times 2^{N_s})$ for an $N_s \times N_s$ matrix. The well-known algorithms for evaluating matrix permanents are the Ryser formula [39–41] and Balasubramanian-Bax-Franklin-Glynn (BBFG) formula [41–45]. For example, in the BBFG algorithm, the permanent for an $n \times n$ matrix (A) is evaluated as

$$\text{perm}A = \frac{1}{2^{n-1}} \sum_{\delta} \left(\prod_{k=1}^n \delta_k \right) \prod_{j=1}^n \sum_{i=1}^n \delta_i a_{ij}. \quad (7)$$

Here, a_{ij} is the element of the matrix A , and the summation is taken over $\delta = (\delta_1, \delta_2, \dots, \delta_n) \in \{\pm 1\}^n$ with $\delta_1 = 1$. The exponential-time cost stems from the fact that the number of terms in the summation grows exponentially in n .

To evaluate the permanent of an $n \times n$ matrix A more efficiently, we propose a random sampling method. Instead of taking all the terms in the summation in Eq. (7), we randomly sample a subset of terms. We replace the sum over the vector δ in Eq. (7) by the random vector r . Note that the equivalent sampling procedure itself is proposed in Ref. [46], although the context is different and the efficiency of the random sampling that we adopt here is not discussed. As we show below, this method allows us to approximately evaluate the permanent with the matrix size larger than 100, which is difficult to achieve with the conventional Ryser and BBFG algorithms.

To simplify the notation, let us introduce the Glynn estimator for an $n \times n$ complex matrix A and the complex vector x [41, 47–49], which is defined as

$$\text{Gly}_x(A) = \prod_{k=1}^n x_k^* \prod_{i=1}^n \left(\sum_{j=1}^n a_{ij} x_j \right). \quad (8)$$

When we specifically choose a random variable r , which has elements $r_i \in \mathbb{C}$ ($i = 1, 2, \dots, n$) that are independently chosen uniformly on $|r_i| = 1$, we can evaluate the permanent of the matrix as the expectation value of the Glynn estimator $\text{Gly}_r(A)$ [41, 47–49]. The relation is given as

$$\text{perm}A = \mathbb{E}[\text{Gly}_r(A)] = \mathbb{E} \left[\prod_{i=1}^n r_i^* \left(\sum_{j=1}^n a_{ij} r_j \right) \right], \quad (9)$$

where \mathbb{E} means the expectation value. We can calculate the permanent by the following sample mean,

$$\text{perm}A \approx \frac{1}{N_{\text{smp}}} \sum_{m=1}^{N_{\text{smp}}} p^{(m)}, \quad (10)$$

$$p^{(m)} = \prod_{i=1}^n r_i^{(m)*} \left(\sum_{j=1}^n a_{ij} r_j^{(m)} \right), \quad (11)$$

where N_{smp} is the number of samples, and $r^{(m)}$ is a complex random vector of a sample m . In practice, we take $r_i^{(m)} =$

$\exp[i\theta_i^{(m)}]$ with $\theta_i^{(m)}$ chosen uniformly in $[0, 2\pi]$ [48–50]. The value $p^{(m)}$ is a complex number for each sample m .

In the present system with $n = N_s$, the entanglement entropy satisfies $0 \leq S_2 \leq cN_s$ with c being a sufficiently large constant, and therefore, the condition $\exp(-cN_s) \leq \text{perm}A \leq 1$ holds. Since $\text{Re } p^{(m)}$ and $\text{Im } p^{(m)}$ can be exponentially small in N_s and can be both positive and negative, we need $N_{\text{smp}} = \mathcal{O}[\exp(\alpha N_s)]$ samples with a constant α to accurately estimate $\text{perm}A$ in general. The situation is similar to the case of systems having the notorious negative sign problems [51]. The advantage of the present approach is that the constant prefactor α would be sufficiently smaller than unity as far as we deal with the matrix A generated in the present system [see Eq. (4)]. Indeed, we have numerically found that $\alpha \approx 0.2$. One may also consider the importance sampling to reduce the variance of the estimator in Eq. (8). However, we do not use it in the present study and stick to the simple random sampling method because we are interested in how far we can go with the primitive procedure. Note that although we here focus on the CDW initial state to be specific, the approach described above is applicable also to other insulating initial states as long as they are expressed as a simple product of local Fock states.

III. RESULTS

Hereafter, we present the numerical results on dynamics of the entanglement entropy in hypercubic lattices, such as a chain in 1D and a square lattice in 2D. The number of sites is given by N_s on a 1D chain and $N_s = L_x \times L_y$ on a 2D square lattice.

A. Estimation of the statistical error

Before estimating the expectation value and the statistical error of $\text{perm}A$ in Eq. (10), we examine the distribution of the value $p^{(m)}$. For simplicity, we will focus on the 1D case for the moment. We specifically consider the system size $N_s = 40$ and investigate the distribution of 2^{20} samples at a short time ($tJ = 1$) and at a long time ($tJ = 2N_s$).

Let us first look into the imaginary part of each sample required for calculating $\text{Im } \text{perm}A$. In the present study, we expect $\text{Im } \text{perm}A = 0$ because $\text{perm}A = \exp(-S_2)$ ($S_2 \in \mathbb{R}$) should be real. As shown in Fig. 1, we examine the distribution of the positive and negative $\text{Im } p^{(m)}$ at a short time $tJ = 1$ and at a long time $tJ = 2N_s$. In each time, the positive and negative components exhibit nearly the same shape and cancel each other out, suggesting that $\text{Im } \text{perm}A = 0$ as expected when the number of samples is sufficiently large. Indeed, we have numerically confirmed that the expectation value of $\text{Im } \text{perm}A$ is always zero within the sufficiently small statistical error.

We then investigate the real part of $\text{perm}A$. As in the case of imaginary part, we examine the distribution of the positive and negative $\text{Re } p^{(m)}$ at a short time $tJ = 1$ and at a long time $tJ = 2N_s$.

In the short time case ($tJ = 1$), we expect $S_2 = \mathcal{O}(1)$ because the entanglement entropy does not grow significantly.

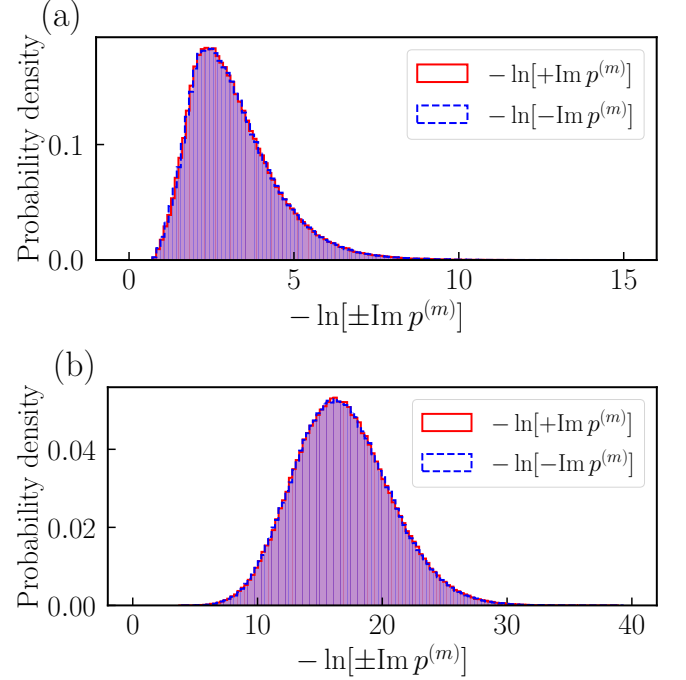


FIG. 1. Distribution of the value $-\ln[\pm \text{Im } p^{(m)}]$ in Eq. (11). We show the distribution $P(x)$ of $x = -\ln[\pm \text{Im } p^{(m)}]$ ($x = -\ln[-\text{Im } p^{(m)}]$ when $\text{Im } p^{(m)} > 0$ ($\text{Im } p^{(m)} < 0$)) with a red solid line (a blue dashed line). (a) At time $tJ = 1$ for $N_s = 40$. (b) At time $tJ = 2N_s$ for $N_s = 40$. In both cases, the positive and negative components exhibit nearly the same distribution, suggesting that $\text{perm}A$ does not contain an imaginary part.

Therefore, the condition $\text{perm}A = \mathcal{O}(1)$ likely holds. As we expected, the distribution of the positive $\text{Re } p^{(m)}$ has much greater weight than the negative one [see Fig. 2(a)]. The positive component has a peak at $\text{Re } p^{(m)} \approx +e^{-1}$, whereas the negative component has a peak at $\text{Re } p^{(m)} \approx -e^{-3}$. Since the distribution is not a normal distribution, we need careful analysis to estimate the statistical error, as we will show later in this section.

On the other hand, in the long time case ($tJ = 2N_s$), we expect $S_2 = \mathcal{O}(N_s)$ since the time-evolved state converges to a highly entangled steady state. Therefore, the condition $\text{perm}A = \mathcal{O}[\exp(-\text{const} \times N_s)]$ likely holds, and the sampling must be much harder than the short time case. Indeed, as shown in Fig. 2(b), the positive and negative distributions exhibit a similar shape, indicating that the expectation value is extremely small. At the same time, the area of the positive distribution is slightly larger than that of the negative one, suggesting that $\text{Re } \text{perm}A > 0$. As in the case of a short time, the distribution of $\text{Re } p^{(m)}$ is not a normal distribution, which can be confirmed by the presence of two peaks at $\text{Re } p^{(m)} \approx \pm e^{-16}$. Therefore, also for the long time case, careful analysis is required to estimate the statistical error.

To estimate the statistical error, we combine the blocking analysis and the bootstrap method. In the blocking analysis, we divide the N_{total} samples into N_{block} blocks containing $N_{\text{blocksize}} = N_{\text{total}}/N_{\text{block}}$ samples. For each block j ($= 1, 2, \dots, N_{\text{block}}$), we calculate the expectation value $\bar{p}^{(j)}$ and the variance σ_j^2 of the samples in the block. The final expectation value \bar{p} and variance σ^2 are given by

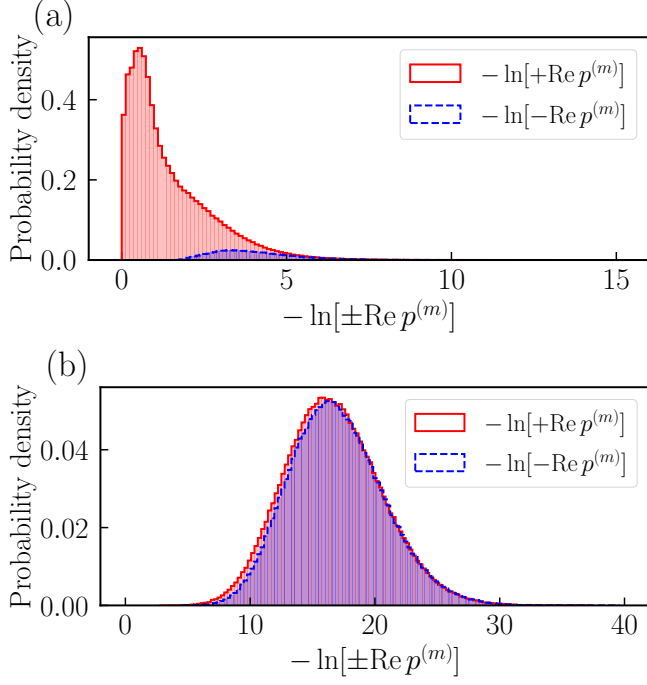


FIG. 2. Distribution of the value $-\ln[\pm \operatorname{Re} p^{(m)}]$ in Eq. (11). We show the distribution $P(x)$ of $x = -\ln[+\operatorname{Re} p^{(m)}]$ ($x = -\ln[-\operatorname{Re} p^{(m)}]$) when $\operatorname{Re} p^{(m)} > 0$ ($\operatorname{Re} p^{(m)} < 0$) with a red solid line (a blue dashed line). (a) At time $tJ = 1$ for $N_s = 40$. Since the positive component is dominant, we expect $\operatorname{perm}A = \mathcal{O}(1)$, and thus, $S_2 = \mathcal{O}(1)$. (b) At time $tJ = 2N_s$ corresponding to $S_2 = \mathcal{O}(N_s)$ for $N_s = 40$. Since the positive and negative components are comparable while the positive one is slightly dominant, we expect $\operatorname{perm}A = \mathcal{O}[\exp(-\text{const} \times N_s)]$, and thus, $S_2 = \mathcal{O}(N_s)$.

2, ..., N_{block}), we calculate average $p^{(j, N_{\text{blocksize}})}$ of $N_{\text{blocksize}}$ samples. This procedure results in

$$\frac{1}{N_{\text{total}}} \sum_{m=1}^{N_{\text{total}}} p^{(m)} = \frac{1}{N_{\text{block}}} \sum_{j=1}^{N_{\text{block}}} p^{(j, N_{\text{blocksize}})}, \quad (12)$$

$$p^{(j, N_{\text{blocksize}})} = \frac{1}{N_{\text{blocksize}}} \sum_{k=(j-1)N_{\text{blocksize}}+1}^{jN_{\text{blocksize}}} p^{(k)}. \quad (13)$$

We then prepare resampled data by the bootstrap method. To this end, we randomly choose N_{block} samples $q^{(j)}$ ($j = 1, 2, \dots, N_{\text{block}}$) from the original N_{block} samples $p^{(j, N_{\text{blocksize}})}$ ($j = 1, 2, \dots, N_{\text{block}}$). Here, we do not avoid picking the same samples multiple times. We repeat this process N_{boot} times and generate samples $\bar{q}^{(k)}$ ($k = 1, 2, \dots, N_{\text{boot}}$) by calculating

$$\bar{q}^{(k)} = \frac{1}{N_{\text{block}}} \sum_{j=1}^{N_{\text{block}}} q^{(j)} \quad (14)$$

for each k . The number N_{boot} is chosen to be sufficiently large so that the resampled data follows a normal distribution. We estimate the average and the standard error of the samples $\bar{q}^{(k)}$, which gives the $\operatorname{perm}A$ and its statistical error $\sigma_{\operatorname{perm}A}$. Then, the statistical error of the Rényi entanglement entropy is

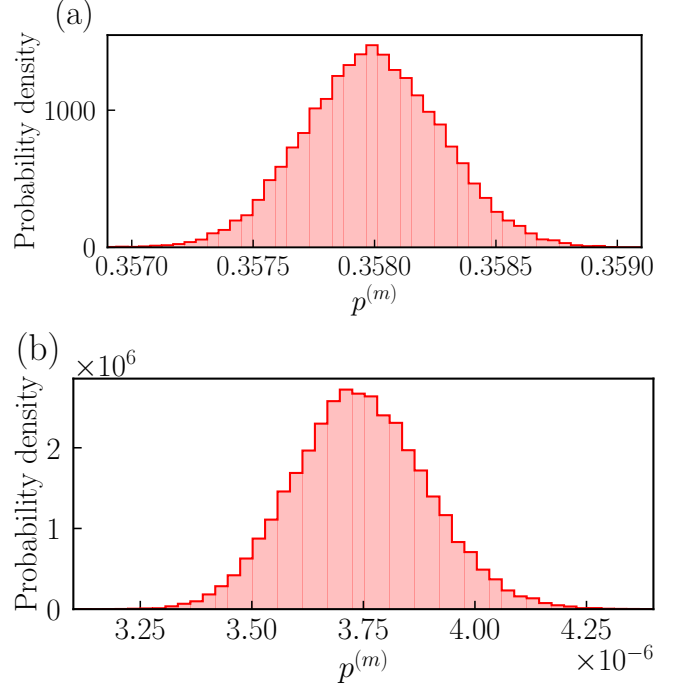


FIG. 3. Estimate of the statistical error using the blocking analysis and the bootstrap method. (a) At time $tJ = 1$ for $N_s = 40$. (b) At time $tJ = 2N_s$ for $N_s = 40$. We choose $N_{\text{total}} = 2^{20}$, $N_{\text{block}} = 2^{10}$, and $N_{\text{boot}} = 2^{12}$. In both cases, the resampled data exhibits a normal distribution, which allows us to estimate the statistical error safely.

evaluated by $\sigma_{S_2} = |-\ln(\operatorname{perm}A + \sigma_{\operatorname{perm}A}) - [-\ln(\operatorname{perm}A)]| \approx |\sigma_{\operatorname{perm}A}/\operatorname{perm}A|$ for $|\sigma_{\operatorname{perm}A}| \ll 1$.

In general, we do not need the blocking analysis; however, the computational cost of the bootstrap method will be extremely high when we directly use the exponentially large number of N_{total} samples. By taking a small constant N_{block} , we can reduce the computational cost of the bootstrap method. Hereafter, we typically choose $N_{\text{block}} = 2^{10}$ and $N_{\text{boot}} = 2^{12}$ and consider exponentially large $N_{\text{total}} \approx \exp(\text{const} \times N_s)$. Note that the period of the pseudorandom number generator should be sufficiently longer than the number of samples. These parameters allow us to safely obtain a normal distribution of the resampled data (for example, see Fig. 3).

B. Size dependence of the statistical error

To estimate the ideal number of samples that we need for each system size, we examine the size dependence of the number of samples under the fixed statistical error. Here, we focus on the 1D system again. For system sizes $N_s = 16, 20, \dots, 60$, we increase the number of samples N_{total} up to 2^{30} and calculate the standard error of the Rényi entanglement entropy density, σ_{S_2/N_s} . The standard error for each system size N_s decreases as

$$\sigma_{S_2/N_s} = \sqrt{\frac{c_{1D}(N_s)}{N_{\text{total}}}} \quad (15)$$

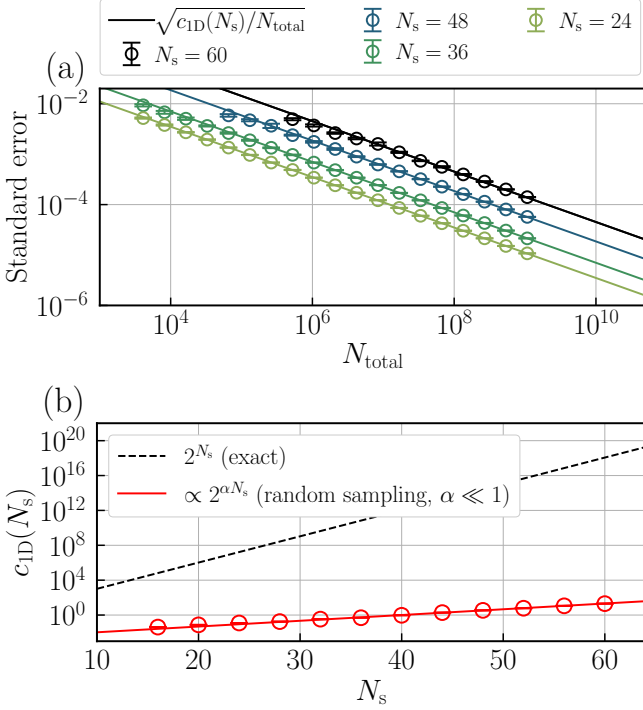


FIG. 4. (a) Size dependence of the standard error of Rényi entanglement entropy density σ_{S_2/N_s} at time $tJ = 2N_s$ as a function of the number of total samples N_{total} in 1D. The statistical error is estimated by the blocking analysis and the bootstrap method with $N_{\text{block}} = 2^{10}$ and $N_{\text{boot}} = 2^{12}$. The error bar of σ_{S_2/N_s} is estimated for 32 independent simulations. The statistical error should satisfy $\sigma_{S_2/N_s} = \sqrt{c_{1D}(N_s)/N_{\text{total}}}$ with $c_{1D}(N_s)$ being a size-dependent constant. (b) Constant $c_{1D}(N_s)$ as a function of size N_s . The value $c_{1D}(N_s)$ represents the number of samples required to achieve a given statistical error σ_{S_2/N_s} . We find that it satisfies $c_{1D}(N_s) \approx 2^{0.2N_s - 9}$ by fitting data for $N_s \geq 40$. It is much smaller than the number of terms (2^{N_s}) in the summation in Eq. (7), suggesting that the computational cost is moderate although it is exponential in N_s .

with increasing N_{total} , where $c_{1D}(N_s)$ is a constant that depends on N_s [see Fig. 4(a)]. The value $c_{1D}(N_s)$ increases exponentially large with increasing system size N_s in general. By fitting numerical data points, we have found

$$c_{1D}(N_s) = 2^{\alpha_{1D} N_s - \beta_{1D}}, \quad (16)$$

$$\alpha_{1D} = 0.219(6), \quad (17)$$

$$\beta_{1D} = 8.8(3), \quad (18)$$

as shown in Fig. 4(b). This result suggests that the number of samples should be

$$N_{\text{total}} = \frac{c_{1D}(N_s)}{(\sigma_{S_2/N_s})^2} \approx \frac{2^{0.2 \times N_s - 9}}{(\sigma_{S_2/N_s})^2} \quad (19)$$

to keep the statistical error σ_{S_2/N_s} constant. When we wish to suppress the statistical error, e.g., $\sigma_{S_2/N_s} = 2^{-10}$, the number of samples should be larger than $N_{\text{total}} = 2^{0.2N_s + 11}$.

The computational cost is proportional to the number of samples and is on the order of $\mathcal{O}(2^{\alpha_{1D} N_s})$ with $\alpha_{1D} \approx 0.2 \ll 1$

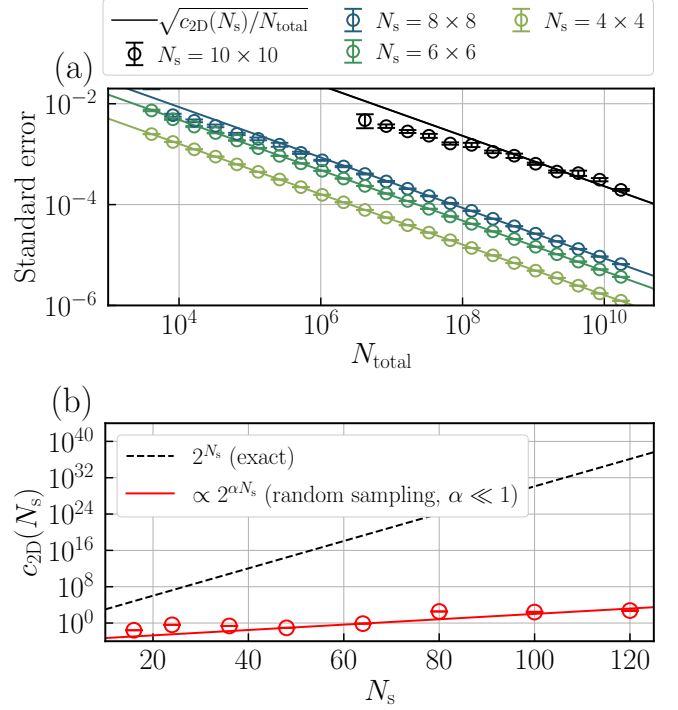


FIG. 5. (a) Size dependence of the standard error of Rényi entanglement entropy density σ_{S_2/N_s} at time $tJ = 2L_x$ as a function of the number of total samples N_{total} in 2D. We consider the lattice sites $N_s = L_x \times L_y$ up to $N_s = 12 \times 10$. The statistical error is estimated by the blocking analysis and the bootstrap method with $N_{\text{block}} = 2^{10}$ and $N_{\text{boot}} = 2^{12}$. The error bar of σ_{S_2/N_s} is estimated for 32 independent simulations. The statistical error should satisfy $\sigma_{S_2/N_s} = \sqrt{c_{2D}(N_s)/N_{\text{total}}}$ with $c_{2D}(N_s)$ being a size-dependent constant. (b) Constant $c_{2D}(N_s)$ as a function of size N_s . We find that it satisfies $c_{2D}(N_s) \approx 2^{0.2N_s - 13}$ by fitting data for $N_s > 40$. As in the case of 1D, the prefactor (≈ 0.2) of N_s in 2D is much smaller than unity, suggesting that the computational cost is moderate although it is exponential in N_s .

in the 1D case. Consequently, the random sampling method is much more efficient than the conventional algorithms in Eq. (7), requiring the summation of 2^{N_s} terms.

The similar small constant prefactor $\alpha_{2D} \approx 0.2$ is also found in the 2D case by analyzing systems up to 120 sites. As shown in Fig. 5(a), we extract the size dependence of the coefficient $c_{2D}(N_s)$ in the fitting function

$$\sigma_{S_2/N_s} = \sqrt{\frac{c_{2D}(N_s)}{N_{\text{total}}}}. \quad (20)$$

We have found that the value $c_{2D}(N_s)$ satisfies

$$c_{2D}(N_s) = 2^{\alpha_{2D} N_s - \beta_{2D}}, \quad (21)$$

$$\alpha_{2D} = 0.20(8), \quad (22)$$

$$\beta_{2D} = 13(4), \quad (23)$$

as shown in Fig. 5(b). Therefore, the computational cost is also on the order of $\mathcal{O}(2^{\alpha_{2D} N_s})$ with $\alpha_{2D} \approx 0.2 \ll 1$ in the 2D case. In practice, as for the system size $N_s = 10 \times 10$ at the time

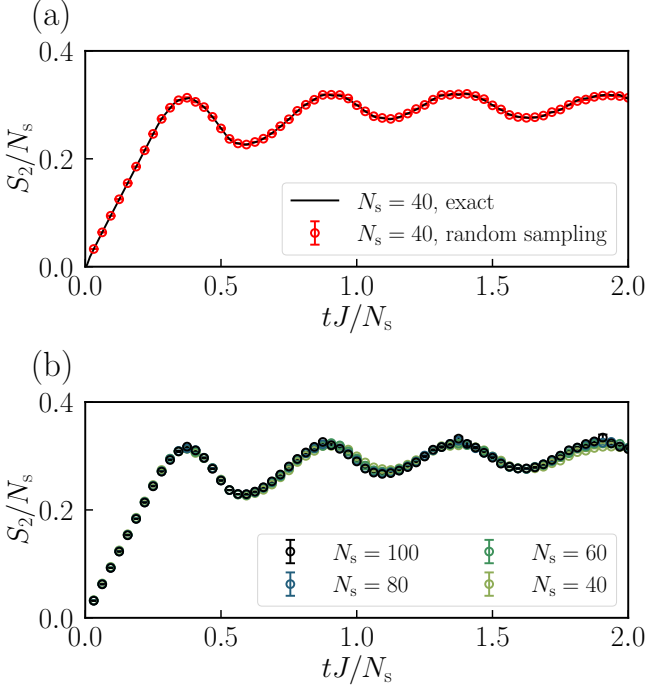


FIG. 6. (a) Comparison with the exact result of the time evolution of the Rényi entanglement entropy density in 1D for $N_s = 40$, which was the largest size obtained by the brute-force computation of the matrix permanent. The results are in good agreement. (b) Time evolution of the Rényi entanglement entropy density for much larger systems.

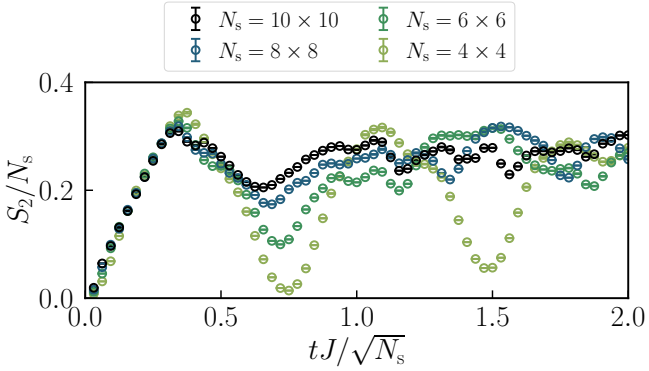


FIG. 7. Time evolution of the Rényi entanglement entropy density in 2D. We consider the lattice sites up to $N_s = 10 \times 10$ and calculate the Rényi entanglement entropy density when the system is divided into identical two parts.

point $tJ = 20$, it takes less than a day to calculate the Rényi entanglement entropy using a single core central processing unit.

C. Entanglement entropy dynamics

By taking advantage of the random sampling method, we calculate the dynamics of Rényi entanglement entropy density

after a sudden quench. Hereafter, we choose the number of samples $N_{\text{total}} = 2^{0.2N_s+12}$ to keep the statistical error sufficiently small.

Let us first compare our present result with the exact one calculated with the largest size $N_s = 40$ in our previous study [30] in the case of 1D. As shown in Fig. 6(a), the random sampling method provides the exact Rényi entanglement entropy density within the statistical error bar.

We then study the larger systems up to $N_s = 100$. As shown in Fig. 6(b), the error bar is sufficiently small for all sizes that we have studied. The Rényi entanglement entropy densities for $N_s \geq 40$ nearly overlap, exhibiting the volume law scaling. Thus, the system size $N_s = 40$, corresponding to the largest size in our previous study, is large enough to capture the nature of the entanglement entropy density dynamics in the thermodynamic limit.

Next, we investigate the Rényi entanglement entropy density dynamics in a 2D square lattices. As shown in Fig. 7, the Rényi entanglement entropy density grows linearly in time for a short time up to $tJ \approx 0.3\sqrt{N_s}$ for $N_s = L_x \times L_y$ with $L_x = L_y$. The behavior is consistent with the prediction from the previous studies on the entanglement entropy density dynamic in integrable systems with the Gaussian initial states [19, 20], although our initial state is not the Gaussian state. The system-size dependence of the entanglement entropy density dynamics is rather small in this time regime. When the time is longer than $tJ \approx 0.3\sqrt{N_s}$, the entanglement entropy density shows a larger size dependence. It is difficult to extract the physically meaningful interpretation of the entanglement entropy density dynamics in the thermodynamic limit. However, as the system size increases, the fluctuation of the entanglement entropy density becomes smaller. The entanglement entropy density appears to converge to a certain value, exhibiting volume-law behavior of the entanglement entropy consistent with the previous studies [19, 20]. Within the system sizes that we have studied, the entanglement entropy density approximately approaches the value close to ≈ 0.3 in both 1D and 2D.

IV. CONCLUSIONS AND OUTLOOK

In conclusion, we studied the dynamics of the Rényi entanglement entropy of insulating initial states in free boson systems. Owing to the non-Gaussian nature of the initial states, the calculation of the entanglement entropy requires the evaluation of the matrix permanent, which has the exponential cost. We developed a random sampling method for evaluating the matrix permanent and found that the computational cost is reduced to $O(2^{\alpha N_s})$ with a small constant $\alpha \approx 0.2 \ll 1$ in 1D and 2D N_s -site systems at half filling. This reduction enables us to study the entanglement entropy dynamics for more than 100 sites in free boson systems.

In the present study, we applied the simple random sampling method to the calculation of the Rényi entanglement entropy. One may consider more sophisticated sampling methods, such as the rejection sampling method [52–54] and the importance sampling method [55–57], to reduce the variance of the estimator for the matrix permanent. The upper and lower bounds

of the entanglement entropy, i.e., the lower and upper bounds of the matrix permanent, would be utilized during such sophisticated sampling. As for the upper bound of the entanglement entropy, the second Rényi entanglement entropy is bounded above by the von Neumann entanglement entropy, and the von Neumann entanglement entropy is bounded above by the von Neumann entanglement entropy of a certain Gaussian state having the same two-point correlation functions as the original state [58, 59]. The entanglement entropy of the Gaussian state can often be calculated efficiently. As for the lower bound of the entanglement entropy, by utilizing the following inequalities [49] for the matrix A that always fulfills $\|A\|_2 = 1$ [30] in Eq. (4),

$$\text{perm}A \leq \mathbb{E} \left[\prod_{i=1}^n \left| r_i^* \left(\sum_{j=1}^n a_{ij} r_j \right) \right| \right] = \mathbb{E} \left[\prod_{i=1}^n \left| \sum_{j=1}^n a_{ij} r_j \right| \right] \quad (24)$$

$$\leq \mathbb{E} \left[\left(\frac{1}{n} \sum_{i=1}^n \left| \sum_{j=1}^n a_{ij} r_j \right| \right)^n \right] \quad (25)$$

$$\leq \mathbb{E} \left[\left(\frac{1}{\sqrt{n}} \sqrt{\sum_{i=1}^n \left| \sum_{j=1}^n a_{ij} r_j \right|^2} \right)^n \right] \quad (26)$$

$$\leq \mathbb{E} [\|A\|_2] = 1, \quad (27)$$

one may consider the entanglement-entropy-like quantities,

$$S'_2 = -\ln \mathbb{E} \left[\prod_{i=1}^n \left| \sum_{j=1}^n a_{ij} r_j \right| \right], \quad (28)$$

$$S''_2 = -\ln \mathbb{E} \left[\left(\frac{1}{n} \sum_{i=1}^n \left| \sum_{j=1}^n a_{ij} r_j \right| \right)^n \right], \quad (29)$$

$$S'''_2 = -\ln \mathbb{E} \left[\left(\frac{1}{\sqrt{n}} \sqrt{\sum_{i=1}^n \left| \sum_{j=1}^n a_{ij} r_j \right|^2} \right)^n \right], \quad (30)$$

satisfying

$$S_2 \geq S'_2 \geq S''_2 \geq S'''_2 \geq 0. \quad (31)$$

The quantities S'_2 , S''_2 , and S'''_2 can be calculated more efficiently than S_2 using the simple random sampling method or the importance sampling method because the quantities inside the expectation operator \mathbb{E} are always nonnegative. When we wish to apply the rejection sampling method, for example, we may utilize the relation between the quantities $p(\mathbf{r}) = \prod_{i=1}^n r_i^* \left(\sum_{j=1}^n a_{ij} r_j \right)$ in Eq. (11) and $q(\mathbf{r}) := \prod_{i=1}^n \left| \sum_{j=1}^n a_{ij} r_j \right|$ that appears in Eq. (28). Since $q(\mathbf{r})$ is always nonnegative and the relation $p(\mathbf{r}) \leq q(\mathbf{r})$ holds for any \mathbf{r} , we can sample the random vector \mathbf{r} from the distribution that generates $q(\mathbf{r})$ using the simple random sampling method and then sample s from the uniform distribution on the interval $[0, q(\mathbf{r})]$. The sample \mathbf{r} is accepted if $s \leq p(\mathbf{r})$ and is rejected

otherwise. One can also combine the rejection and importance sampling methods [60]. The negative-sign-problem-like difficulty would be slightly alleviated when $p(\mathbf{r})$ is close to $q(\mathbf{r})$ for \mathbf{r} that is likely to be sampled.

Although we specifically focused on the 010101 \cdots -type CDW initial state, our approach can apply to other initial states that can be represented by a simple product of local Fock states. We expect that the computational cost of the random sampling method does not significantly depend on the details of the initial states. When the initial state contains N_b particles, we need to evaluate the permanent of an $N \times N$ matrix with $N = 2N_b$ to calculate the entanglement entropy. We speculate that the factor α in the computational cost $\mathcal{O}(2^{\alpha N})$ of the random sampling method would be primarily determined by the size of the entanglement entropy per particle. This is because when the entanglement entropy per particle s is small and close to zero, the sample $\text{Re } p^{(m)} [\approx \exp(-sN)]$ in Eq. (11) should be close to unity for most samples m , indicating that the most of the samples are positive [see Fig. 2(a) as an example in the case of $s \approx 0$]. Consequently, the sampling efficiency increases and the factor α decreases, irrespective of the choice of the initial state as long as the entanglement entropy per particle is s . In the worst case, the number of samples required to achieve a given statistical error is equivalent to the number of terms in the summation that appears in the BBFG formula in Eq. (7), which suggests $\alpha = 1$. In practice, the factor α would be smaller than unity because the entanglement entropy per particle is on the order of $\mathcal{O}(1)$ in physically relevant systems. Indeed, the factor is $\alpha \approx 0.2 \ll 1$ when the entanglement entropy per particle is $s \approx 2 \times 0.3$ in the present 1D and 2D systems. It is intriguing to explore how the computational cost of the random sampling method depends on the entanglement entropy per particle in various initial states.

We specifically studied the dynamics of the Rényi entanglement entropy in free boson systems after a sudden quench. One may also consider the problems in the boson sampling devices [48, 61]. There are several proposals for reducing the computational cost of the matrix permanent regarding the boson sampling procedure [62, 63]. In practice, the feasible matrix size is up to $\approx 50 \times 50$ so far [64–66]. It is an interesting problem to study whether the sampling method also reduces the computational cost of the permanent of the matrix representing the boson sampling task.

As for the dynamics in the presence of interactions, namely, the dynamics in the Bose-Hubbard model, the information propagation and the particle transport would behave differently [67]. The former speed could be much faster than the latter speed. Since the numerical investigation of the entanglement entropy dynamics in strongly correlated systems is much more challenging, studying the dynamics in noninteracting boson systems using the random sampling method would help understand the information propagation in nonequilibrium quantum systems.

ACKNOWLEDGMENTS

The authors acknowledge fruitful discussions with Shimei Goto, Kota Sugiyama, Yuki Takeuchi, Shunji Tsuchiya, Shion Yamashika, and Ryosuke Yoshii. This work was supported by JSPS KAKENHI (Grant No. JP24H00973), MEXT KAKENHI, Grant-in-Aid for Transformative Research Area

(Grants No. JP22H05111 and No. JP22H05114), JST FOREST (Grant No. JPMJFR202T), and MEXT Q-LEAP (Grant No. JPMXS0118069021). The numerical computations were performed on computers at the Yukawa Institute Computer Facility, Kyoto University and on computers at the Supercomputer Center, the Institute for Solid State Physics, the University of Tokyo.

[1] M. Greiner, O. Mandel, T. Esslinger, T. W. Hänsch, and I. Bloch, *Nature* **415**, 39 (2002).

[2] P. Calabrese and J. Cardy, *J. Stat. Mech.* **2005**, P04010 (2005).

[3] G. D. Chiara, S. Montangero, P. Calabrese, and R. Fazio, *J. Stat. Mech.* **2006**, P03001 (2006).

[4] M. Cramer, C. M. Dawson, J. Eisert, and T. J. Osborne, *Phys. Rev. Lett.* **100**, 030602 (2008).

[5] M. Cramer, A. Flesch, I. P. McCulloch, U. Schollwöck, and J. Eisert, *Phys. Rev. Lett.* **101**, 063001 (2008).

[6] A. Flesch, M. Cramer, I. P. McCulloch, U. Schollwöck, and J. Eisert, *Phys. Rev. A* **78**, 033608 (2008).

[7] M. Fagotti and P. Calabrese, *Phys. Rev. A* **78**, 010306 (2008).

[8] A. M. Läuchli and C. Kollath, *J. Stat. Mech.* **2008**, P05018 (2008).

[9] J. Eisert, M. Cramer, and M. B. Plenio, *Rev. Mod. Phys.* **82**, 277 (2010).

[10] P. Barmettler, D. Poletti, M. Cheneau, and C. Kollath, *Phys. Rev. A* **85**, 053625 (2012).

[11] J. H. Bardarson, F. Pollmann, and J. E. Moore, *Phys. Rev. Lett.* **109**, 017202 (2012).

[12] M. Cheneau, P. Barmettler, D. Poletti, M. Endres, P. Schauß, T. Fukuhara, C. Gross, I. Bloch, C. Kollath, and S. Kuhr, *Nature* **481**, 484 (2012).

[13] S. Trotzky, Y.-A. Chen, A. Flesch, I. P. McCulloch, U. Schollwöck, J. Eisert, and I. Bloch, *Nat. Phys.* **8**, 325 (2012).

[14] G. Carleo, F. Becca, L. Sanchez-Palencia, S. Sorella, and M. Fabrizio, *Phys. Rev. A* **89**, 031602 (2014).

[15] A. Bauer, F. Dorfner, and F. Heidrich-Meisner, *Phys. Rev. A* **91**, 053628 (2015).

[16] I. Frerot and T. Roscilde, *Phys. Rev. B* **92**, 115129 (2015).

[17] I. Frerot and T. Roscilde, *Phys. Rev. Lett.* **116**, 190401 (2016).

[18] N. Laflorencie, *Phys. Rep.* **646**, 1 (2016).

[19] V. Alba and P. Calabrese, *Proc. Natl. Acad. Sci. U.S.A.* **114**, 7947 (2017).

[20] V. Alba and P. Calabrese, *SciPost Phys.* **4**, 017 (2018).

[21] S. Goto and I. Danshita, *Phys. Rev. B* **99**, 054307 (2019).

[22] K. Nagao, M. Kunimi, Y. Takasu, Y. Takahashi, and I. Danshita, *Phys. Rev. A* **99**, 023622 (2019).

[23] R. Yao and J. Zakrzewski, *Phys. Rev. B* **102**, 104203 (2020).

[24] Y. Takasu, T. Yagami, H. Asaka, Y. Fukushima, K. Nagao, S. Goto, I. Danshita, and Y. Takahashi, *Sci. Adv.* **6**, eaba9255 (2020).

[25] M. Kunimi and I. Danshita, *Phys. Rev. A* **104**, 043322 (2021).

[26] K. Nagao, Y. Takasu, Y. Takahashi, and I. Danshita, *Phys. Rev. Research* **3**, 043091 (2021).

[27] R. Yoshii, S. Yamashika, and S. Tsuchiya, *J. Phys. Soc. Jpn.* **91**, 054601 (2022).

[28] C. Rylands, B. Bertini, and P. Calabrese, *J. Stat. Mech.* **2022**, 103103 (2022).

[29] R. Kaneko and I. Danshita, *Commun. Phys.* **5**, 65 (2022).

[30] D. Kagamihara, R. Kaneko, S. Yamashika, K. Sugiyama, R. Yoshii, S. Tsuchiya, and I. Danshita, *Phys. Rev. A* **107**, 033305 (2023).

[31] S. Yamashika, D. Kagamihara, R. Yoshii, and S. Tsuchiya, *Phys. Rev. Res.* **5**, 043102 (2023).

[32] S. Yamashika, P. Calabrese, and F. Ares, *arXiv:2410.14299*.

[33] D. A. Abanin and E. Demler, *Phys. Rev. Lett.* **109**, 020504 (2012).

[34] A. J. Daley, H. Pichler, J. Schachenmayer, and P. Zoller, *Phys. Rev. Lett.* **109**, 020505 (2012).

[35] A. Elben, B. Vermersch, M. Dalmonte, J. I. Cirac, and P. Zoller, *Phys. Rev. Lett.* **120**, 050406 (2018).

[36] R. Islam, R. Ma, P. M. Preiss, M. Eric Tai, A. Lukin, M. Rispoli, and M. Greiner, *Nature* **528**, 77 (2015).

[37] A. M. Kaufman, M. E. Tai, A. Lukin, M. Rispoli, R. Schittko, P. M. Preiss, and M. Greiner, *Science* **353**, 794 (2016).

[38] T. Brydges, A. Elben, P. Jurcevic, B. Vermersch, C. Maier, B. P. Lanyon, P. Zoller, R. Blatt, and C. F. Roos, *Science* **364**, 260 (2019).

[39] H. J. Ryser, *Combinatorial mathematics*, Vol. 14 (American Mathematical Soc., 1963).

[40] R. A. Brualdi and H. J. Ryser, *Combinatorial matrix theory* (Cambridge University Press, 1991).

[41] D. G. Glynn, *Eur. J. Combinat.* **31**, 1887 (2010).

[42] K. Balasubramanian, *Combinatorics and diagonals of matrices*, Ph.D. thesis, Indian Statistical Institute-Kolkata (1980).

[43] E. Bax and J. Franklin, CalTech-CS-TR-96-04 (1996).

[44] E. T. Bax, *Finite-difference algorithms for counting problems* (California Institute of Technology, 1998).

[45] D. G. Glynn, *Des. Codes Cryptogr.* **68**, 39 (2013).

[46] J. Huh, *arXiv:2205.01328*.

[47] L. Gurvits, in *Mathematical Foundations of Computer Science 2005*, edited by J. Jędrzejowicz and A. Szepietowski (Springer Berlin Heidelberg, Berlin, Heidelberg, 2005) pp. 447–458.

[48] S. Aaronson and T. Hance, *Quantum Inf. Comput.* **14**, 541 (2014).

[49] R. Berkowitz and P. Devlin, *Isr. J. Math.* **224**, 437 (2018).

[50] V. Kocharovskiy, V. Kocharovskiy, and S. Tarasov, *Entropy* **22**, 322 (2020).

[51] E. Y. Loh, J. E. Gubernatis, R. T. Scalettar, S. R. White, D. J. Scalapino, and R. L. Sugar, *Phys. Rev. B* **41**, 9301 (1990).

[52] M. Huber and J. Law, in *Proceedings of the Nineteenth Annual ACM-SIAM Symposium on Discrete Algorithms*, SODA '08 (Society for Industrial and Applied Mathematics, USA, 2008) pp. 681–689.

[53] J. Kuck, T. Dao, H. Rezatofighi, A. Sabharwal, and S. Ermon, in *Advances in Neural Information Processing Systems*, Vol. 32, edited by H. Wallach, H. Larochelle, A. Beygelzimer, F. d'Alché-Buc, E. Fox, and R. Garnett (Curran Associates, Inc., 2019).

[54] J. Harviainen, A. Röyskö, and M. Koivisto, in *Advances in Neural Information Processing Systems*, Vol. 34, edited by M. Ranzato, A. Beygelzimer, Y. Dauphin, P. Liang, and J. W. Vaughan (Curran Associates, Inc., 2021) pp. 213–224.

[55] M. Jerrum, A. Sinclair, and E. Vigoda, *J. ACM* **51**, 671 (2004).

- [56] I. Bezákova, D. Štefankovič, V. V. Vazirani, and E. Vigoda, *SIAM J. Comput.* **37**, 1429 (2008).
- [57] S. C. Kou and P. McCullagh, *Biometrika* **96**, 635 (2009).
- [58] E. Bianchi, L. Hackl, and N. Yokomizo, *J. High Energ. Phys.* **2018** (03), 1.
- [59] L. Hackl, E. Bianchi, R. Modak, and M. Rigol, *Phys. Rev. A* **97**, 032321 (2018).
- [60] J. S. Liu, R. Chen, and W. H. Wong, *J. Am. Stat. Assoc.* **93**, 1022 (1998).
- [61] S. Aaronson and A. Arkhipov, in *Proceedings of the forty-third annual ACM symposium on Theory of computing* (2011) pp. 333–342.
- [62] N. Quesada, R. S. Chadwick, B. A. Bell, J. M. Arrazola, T. Vincent, H. Qi, and R. García–Patrón, *PRX Quantum* **3**, 010306 (2022).
- [63] P. Clifford and R. Clifford, *Phys. Scr.* **99**, 065121 (2024).
- [64] A. Neville, C. Sparrow, R. Clifford, E. Johnston, P. M. Birchall, A. Montanaro, and A. Laing, *Nat. Phys.* **13**, 1153 (2017).
- [65] J. Wu, Y. Liu, B. Zhang, X. Jin, Y. Wang, H. Wang, and X. Yang, *Natl. Sci. Rev.* **5**, 715 (2018).
- [66] P.-H. Lundow and K. Markström, *J. Comput. Phys.* **455**, 110990 (2022).
- [67] T. Kuwahara, T. V. Vu, and K. Saito, *Nat. Commun.* **15**, 2520 (2024).